HHS Public Access

Author manuscript

J Inorg Biochem. Author manuscript; available in PMC 2015 July 28.

Published in final edited form as:

J Inorg Biochem. 2014 July ; 136: 115–121. doi:10.1016/j.jinorgbio.2014.01.014.

Toxic Metal Proteomics: Reaction of the Mammalian Zinc Proteome with Cd^{2+}

Mohammad Ali Namdarghanbari, **Joseph Bertling**, **Susan Krezoski**, and **David H. Petering***

Department of Chemistry and Biochemistry, University of Wisconsin-Milwaukee, Milwaukee, Wisconsin USA 53201

Abstract

The hypothesis was tested that Cd^{2+} undergoes measureable reaction with the Zn-proteome through metal ion exchange chemistry. The Zn-proteome of pig kidney $LLCPK_1$ cells is relatively inert to reaction with competing ligands, including Zinquin acid, EDTA, and apo-metallothionein. Upon reaction of Cd^{2+} with the Zn-proteome, Cd^{2+} associates with the proteome and near stoichiometric amounts of Zn^{2+} become reactive with these chelating agents. The results strongly support the hypothesis that Cd^{2+} displaces Zn^{2+} from native proteomic binding sites resulting in the formation of a Cd-proteome. Mobilized Zn^{2+} becomes adventitiously bound to proteome and available for reaction with added metal binding ligands. Cd-proteome and Zn-metallothionein readily exchange metal ions, raising the possibility that this reaction restores functionality to Cd-proteins. In a parallel experiment, cells were exposed to Cd^{2+} and pyrithione briefly to generate substantial proteome-bound Cd^{2+}. Upon transition to a Cd^{2+} free medium, the cells generated new metallothionein protein over time that bound most of the proteomic Cd^{2+} as well as additional Zn^{2+}.

Keywords

zinc proteome; cadmium; metallothionein; metal exchange

1. Introduction

Understanding how toxic metal ion (M^{n+}) cause cell injury requires that the intracellular sites of binding that cause the underlying changes in cell biochemistry be determined [1]. Considering the plethora of metal binding groups that adorn proteins (carboxylate, amine, thiolate, imidazole), nucleic acids (phosphate esters, purine and pyrimidine bases), and small molecules (e.g. glutathione thiol, carboxyl, and amine groups), multiple metal binding interactions can be proposed, in which L represents these ligands:

*Address correspondence to: David H. Petering, Department of Chemistry and Biochemistry, University of Wisconsin-Milwaukee, petering@uwm.edu, 414-229-5530.

$$M^{n+}+L_1 \rightleftarrows M-L_1; M-L_1+L_2 \rightleftarrows M-L_2+L_1; M-L_{n-1}+L_n \rightleftarrows M-L_n+L_{n-1} \quad (1)$$

Despite decades of research into the biological toxicology of many metallic species, few sites have been identified that are causally linked to toxicity (e.g. M-L_n). In the case of Cd^{2+}, the principal binding site that has dominated studies of this metal ion is metallothionein (MT) [2]. Among various functions, MT serves as a means of protection against this and other metal ions.

Cd^{2+} exposure causes the loss of function of a suite of Na^+-dependent nutrient transporters in the kidney [3,4]. Recently, the Zn-finger transcription factor, Zn_3-Sp1 has been shown to be the target of reaction with Cd^{2+} that leads to the down regulation of Na^+-dependent glucose transporter mRNA and protein expression in the kidney proximal tubule [5,6]. In turn, cells lose their ability to transport glucose, a hallmark of human and rodent Cd^{2+} toxicity [7,8]. Direct metal ion exchange has been observed *in vitro* that may result in a rearrangement of finger structure and fully destroys function [9]:

$$Zn_3-Sp1+3Cd^{2+} \rightleftarrows Cd_3-Sp1+3Zn^{2+}; Cd_3-Sp1 \rightleftarrows Cd_{3-n}-Sp1'+nCd^{2+} \quad (2)$$

Cd^{2+} causes a variety of other pathological effects in cultured cells [10,11]. Surely, all of these changes cannot be ascribed to reaction of Cd^{2+} with Zn_3-Sp1 alone. Zn_3-Sp1 is a member of the most common type of Zn-finger structure that contains Zn^{2+} binding sites involving two cysteine sulfhydryl and two histidine imidazole ligands [12,13]. There are hundreds of such proteins in mammalian cells and it may be expected that many react with Cd^{2+} as does Zn_3-Sp1 [14]. Thus, to fully understand the determinants of toxicity, a proteomic approach is necessary, in which a number of sites may contribute to cell injury [15]. This paper begins a series of communications about new approaches to doing toxic metal proteomics.

2. Materials and Methods

2.1. Chemicals

Zinquin acid (ZQ) was purchased from Enzo Life Sciences (Plymouth Meeting, PA). The fluorophore was solubilized in DMSO and kept in the dark at 4 °C. Sephadex G-75 gel filtration chromatography beads were purchased from GE Healthcare Bio-Sciences AB. All other chemicals were purchased from Sigma-Aldrich or Fisher Chemical Companies and were reagent grade or highest purity available.

2.2. Cell culture

LLC-PK_1 pig renal epithelial cells were purchased from the American Tissue Culture Company (ATCC CL101). Cells were grown in M199-Hepes culture media supplemented with 4% fetal calf serum (FCS), 50,000 units/l Penicillin, and 50mg/l Streptomycin and with 5% CO_2 and 100% humidity at 37 °C.

2.3. Preparation of cell supernatant and proteome

Cells grown on 100mm diameter culture plates were rinsed three times with cold phosphate buffered saline (PBS) solution. Cells were scraped gently with a rubber cell scrapper and transferred to the cold (4 °C) Dulbecco's phosphate buffered saline (DPBS) solution in a 50 ml centrifuge tube. Cells were then centrifuged at 640 × g for 4 minutes. The resulting cell pellet was transferred to a 12 × 80 mm thin walled tube with 4 mL of cold DPBS and recentrifuged at 1200 × g for 3 min. The supernatant was removed and 1 ml of cold Milli-Q (18MΩ resistant) purified water added. The suspension was sonicated at a power setting of 5 and a 40% pulse using the macro tip for 60 pulses. Cell supernatant was prepared by centrifugation of the sonicated mixture at 47000 × g for 20 min. at 4 °C. Supernatant was loaded onto a 0.7 cm × 80 cm Sephadex G-75 column equilibrated with degassed 20 mM Tris, 0.1 M KCl buffer, pH 7.4. Eluted fractions (1 ml) in the high molecular weight part of the separation profile were pooled, concentrated and designated as the proteome.

2.4. Treatment of supernatant and proteome with Zn^{2+} and Cd^{2+}, gel filtration chromatography, and metal analysis

$CdCl_2$ or $ZnCl_2$ were reacted with cell supernatant and proteome for 60 min at room temperature. The mixture was loaded onto a Sephadex G-75 column as above. Fractions (1 ml) corresponding to high molecular weight proteins were collected and concentrated using an Amicon filtration device with 30 kDa cut off membrane. Concentrated Zn- or Cd-loaded proteome was either reacted immediately with competing ligands or stored in -80 °C for later use. Metal content of fractions was quantified using atomic absorption spectrophotometry (GBC 904) or inductively coupled plasma mass spectrometry (ICP-MS) (Micromass Platform). Chromatographic results presented in the Figures are representative of at least 3 experiments.

2.5. Preparation and characterization of Zn_7-MT and apo-MT

These proteins were prepared as described elsewhere [16]. For this study, rabbit liver MT-2 was used. It was fully characterized by metal, sulfhydryl, and protein analysis as Zn_7-MT. The concentration of apo-MT was calculated as 7/20 of it thiol concentration. The rabbit MT-2 proteins have amino acid sequences that are nearly identical to that of porcine metallothionein, including invariant cysteine positioning and, in contrast to the pig proteins, have been extensively studied [2,17,18].

2.6. Cadmium pyrithione treatment of cell culture

Cells were exposed to 3 μM pyrithione and 60 μM $CdCl_2$ for 30 min. Media was then removed and cells were washed 3 times with cold DPBS and either harvested for analysis or incubated for 6 h and 24 h in fresh media and FCS for further study. Cell supernatant was prepared using the above-mentioned procedure. Sephadex G-75 chromatography was employed as above to isolate the proteome from cell supernatant.

2.7. Fluorescence spectrophotometry

Fluorescence measurements were carried out on a Hitachi F-4500 fluorimeter. The excitation wavelength for Zinquin acid (ZQ) was 370 nm and emission spectra were

obtained over the spectral range of 400 to 600 nm. All fluorescence spectra were recorded in arbitrary units at room temperature and corrected for the background fluorescence

3. Results

The hypothesis tested was that native Zn^{2+} binding sites within the proteome serve as major targets of reaction of Cd^{2+}. Upon reaction, Cd^{2+} would displace Zn^{2+} and occupy a set of such binding sites. Collectively, these reactions can be described as

$$\Sigma\mathrm{Zn-protein_n}+\mathrm{Cd^{2+}} \rightleftarrows \Sigma\mathrm{Cd-protein_n}+\mathrm{Zn^{2+}} \quad (3)$$

or they can be simplified by aggregating the sum of the reactive Zn-protein sites within the proteome as Zn-proteome:

$$\mathrm{Zn-proteome}+\mathrm{Cd^{2+}} \rightleftarrows \mathrm{Cd-proteome}+\mathrm{Zn^{2+}} \quad (4)$$

The alternative hypothesis is that Cd^{2+} associates with other binding sites within the proteome as in reaction 1:

$$\mathrm{Zn-proteome}+\mathrm{Cd^{2+}} \rightleftarrows \mathrm{Zn-proteome \bullet Cd} \quad (5)$$

Reaction of Cd^{2+} with proteome

Proteome from pig kidney LLC-PK_1 cells was isolated by Sephadex G-75 chromatography and analyzed for Zn^{2+} by ICP-MS (Figure 1a). A single band of high molecular weight Zn^{2+} constituted the proteome; no evidence of Zn-metallothionein was obtained (see arrow for location of Zn-MT). To 28 μM Zn^{2+} present as Zn-proteome, as isolated in Figure 1a and reconcentrated, 23 μM Cd^{2+} was added. Following gel filtration chromatography, all of the original Zn^{2+} in the sample plus the added Cd^{2+} migrated with the proteome (Figure 1b). No Cd-MT was observed. This result was consistent with reaction 4, assuming that the displaced Zn^{2+} binds to proteomic ligands. The data in Figure 1b were also in agreement with reaction 5. Thus, other experiments were needed to determine the nature of the reactions that had occurred.

Properties of the Zn-proteome

Properties of the native Zn-proteome in Figure 1a were determined as baseline information about the behavior of native-bound Zn^{2+} within the proteome. Incubation of 10 μM Zn-proteome with the 50 μM ZQ, a Zn^{2+} sensor, for 30 min followed by Sephadex chromatography revealed a small band of low molecular weight Zn^{2+} that was assumed to be $Zn(ZQ)_2$ (7 % of proteomic Zn^{2+}) (Figure 2). Upon addition of Zn^{2+} to Zn-proteome to form Zn-proteome•Zn, ZQ mobilized 60% of the extra Zn^{2+} as $Zn(ZQ)_2$, which was identified by its fluorescence emission spectrum centered at 490 nm [19]. The reaction leading to the increased formation of $Zn(ZQ)_2$ is described by reaction 6:

$$\mathrm{Zn-proteome \bullet Zn}+2\mathrm{ZQ} \rightleftarrows \mathrm{Zn-proteome}+\mathrm{Zn(ZQ)_2} \quad (6)$$

ZQ has a substantial, 2:1 (ligand to metal) stability constant for Zn^{2+} at pH 7 of 10^{13} [20]. For kinetic or thermodynamic reasons, it is largely unreactive with proteomic Zn^{2+} bound to native proteins. It does compete for much of the adventitiously bound Zn^{2+} to form $Zn(ZQ)_2$ and also appears to bind the rest in the form of ternary complexes, which are revealed by a blue-shift in the fluorescence emission spectrum of $Zn(ZQ)_2$ from 490 nm to 470 nm [19]:

$$\mathrm{Zn-proteome \bullet Zn + 2ZQ \rightleftarrows ZQ-Zn-proteome \bullet Zn-ZQ} \quad (7)$$

Also, as documented in previous studies and below in Figure 5a, 4 μM apometallothionein, which provided 28 μM in Zn^{2+} binding sites, removed little if any Zn^{2+} from 28 μM Zn-proteome to form Zn-MT [21,22]. Thus, as with ZQ, Zn-proteome is mostly unreactive with an endogenous ligand, apo-MT, that also has a large binding constant for Zn^{2+}, $10^{11.2}$ [16].

Reaction of Cd^{2+}-treated Zn-proteome with ZQ

Zn-proteome containing 4.5 μM Zn^{2+} and 3.2 μM Cd^{2+} was reacted with 15 μM ZQ in order to determine whether Cd^{2+} had mobilized Zn^{2+} from its proteomic binding sites. According to Figure 3a, the presence of Cd^{2+} increased the emission intensity of ZQ fluorescence above control levels by 2.5 fold and shifted its wavelength maximum from 470 nm toward 480 nm, suggestive of the formation of Zn- or $Cd(ZQ)^2$ which have emission maxima at 490 nm. Upon centrifugal filtration of the reaction mixture to separate proteomic and low molecular weight forms of Zn^{2+}, 25% of the Zn^{2+} originally bound to the proteome (1.1 μM) appeared in the filtrate. Cd^{2+} was not detected in this isolate by atomic absorption spectrophotometry. The fluorescence spectrum of the filtrate displayed a wavelength maximum of 490 nm (Figure 3b), consistent with the presence of $Zn(ZQ)_2$. Remaining in the retentate was protein-bound Zn^{2+} and Cd^{2+}, characterized by a fluorescence spectrum centered at 470 nm (Figure 3b) with much greater intensity than that of the original ZQ-Zn-proteome (Figure 3a, control). As expected, the total fluorescence intensity of separated filtrate and retentate were equal to the initial reaction mixture.

The implication of these results was that Cd^{2+} had initially displaced Zn^{2+} from some of its proteomic binding sites (reaction 4). Cd-proteins can form fluorescent ZQ-Cd-proteins with fluorescence spectral maxima similar to but substantially less intense than those of ZQ-Zn-proteins (data not shown). Possibly, ZQ-Cd-proteome structures may have been generated *in situ*. Moreover, proteome•Zn-ZQ adducts might account for much of the enhanced fluorescence, considering in control experiments that ZQ only mobilized 60% of the adventitiously bound Zn^{2+}. Thus, the contributions that various products made to the fluorescence spectrum of the retentate remained ambiguous.

Reaction of Cd^{2+}-treated proteome with EDTA

Another metal binding ligand, EDTA, was employed to probe the proteome modified by Cd^{2+}. A previous study had shown that under approximately stoichiometric conditions EDTA reacts with LLC-PK_1 Zn-proteome to extract about 30% of its Zn^{2+} [22]. That result was repeated in the present experiment. Upon reaction of Zn-proteome (44 μM) with Cd^{2+} (22 μM), the product was incubated with 86 μM EDTA for 60 min and chromatographed over Sephadex G-75 (Figure 4). The distribution of Zn^{2+} and Cd^{2+} within the effluent

fractions showed that 60 % of the proteomic Zn^{2+} and Cd^{2+} were shifted into the low molecular weight region in association with EDTA. The increased lability of Zn^{2+} was attributed to reaction 4, consistent with the results obtained with ZQ. Appearance of low molecular weight Cd^{2+} meant that some but not all of the proteome-bound Cd^{2+} was also reactive with EDTA.

Reaction of Cd^{2+}-treated Zn-proteome with apo-MT

The reactivity of the Cd^{2+} treated Zn-proteome was then probed with apo-MT. In this case, apo-MT served as the special, strong metal-binding ligand that is induced within cells upon exposure to Cd^{2+} [2]. Thus, apo-MT, which provides 28 μM Cd^{2+} or Zn^{2+} binding sites, was incubated in an anaerobic cell under nitrogen with the product of the reaction of Cd^{2+} (25 μM) with Zn-proteome (44 μM). After 60 min the mixture was chromatographed over Sephadex G-75. According to Figure 5b, apo-MT became fully saturated with metals as it sequestered 70% of the protein-bound Cd^{2+} (15 μM) and a nearly equivalent concentration of Zn^{2+} (14 μM). A minor fraction of the originally added Cd^{2+} remained bound to the proteome. These results were consistent with the conclusion that upon reaction with Zn-proteome, Cd^{2+} displaced Zn^{2+} in approximate 1 to 1 fashion. Subsequently, apo-MT garnered the liberated Zn^{2+} and also competed successfully for most of the Cd^{2+} that was presumably bound to native Zn^{2+} binding sites. In contrast to ZQ, which only captured labile Zn^{2+}, apo-MT managed to bind both adventitious Zn^{2+} and Cd^{2+} that is hypothesized to occupy native Zn^{2+} binding sites.

$$\mathrm{Cd-protome \bullet Zn + apo-MT \rightleftarrows proteome + Cd,Zn-MT} \quad (8)$$

These findings support the hypothesis that Cd^{2+} reacts with the Zn-proteome as shown in reaction 4. They also provide singular evidence that apo-MT can serve as a highly effective competing ligand for Cd^{2+} bound as Cd-protome.

Reaction of Cd^{2+}-treated Zn-proteome with Zn-MT

The cellular reaction of Cd^{2+} with the Zn-proteome was further probed with Zn_7-MT. The intent was to extend the results obtained with apo-MT to the principal metallo-form of MT that is found in cells. During a 30 min incubation of the reaction mixture with Zn-MT, the more complicated exchange of Cd^{2+} and Zn^{2+} between Cd-proteome•Zn and Zn-MT occurred with 1 to 1 stoichiometry with 18.2 μM Zn^{2+} shifting from Zn^7-MT into the proteome band as 18.5 μM Cd^{2+} moved from the proteome into MT (Figure 6).

Based on the quantitative exchange of Cd^{2+} and Zn^{2+}, it is possible that MT mediated both the removal of Cd^{2+} from native protein binding sites and its replacement by Zn^{2+}. If so, then, the long proposed hypothesis gains support that Zn-MT provides Zn^{2+} to reconstitute native Zn-protein functions as it displaces Cd^{2+} from these modified proteins [23]:

$$\mathrm{Cd-proteome \bullet Zn + Zn-MT \rightleftarrows Zn-proteome \bullet Zn + Cd-MT} \quad (9)$$

Reaction of cell supernatant with Cd^{2+}

The cell supernatant differs from proteome in that it contains low molecular weight molecules as well as proteins. Principally, with respect to metal binding, it contributes a large concentration of glutathione, thought to be important in Cd^{2+} trafficking [24]. Cd^{2+} was reacted with lysate under conditions similar to those used for the reactions with Zn-proteome. As with Zn-proteome alone, Cd^{2+} reacted exclusively with the proteome; glutathione did not bind to a measureable fraction of the added metal ion (data not shown).

Time-dependent reaction of cells with $Cd(pyrithione)_2$

The *in vitro* experiments described above demonstrate that upon contact, Cd^{2+} displaces Zn^{2+} from native Zn-protein binding sites and that both apo- and Zn-MT can compete to remove Cd^{2+} from these sites. This provides a model for the cellular behavior of Cd^{2+}. To test this model in cells, the uptake of Cd^{2+} had to be uncoupled from its subsequent reactions with cellular components. Thus, instead of treating cells with Cd^{2+} for a lengthy time period such as 24 h, during which many reactions between Cd^{2+} and cell constituents might occur, cells were exposed for 30 min to Cd^{2+} and then allowed to respond over time in the absence of further exposure.

LLC-PK_1 cells (ca. 10^8) were incubated with 60 μM Cd^{2+} in the presence of 3 μM pyrithione for 30 min to effect rapid intracellular accumulation of Cd^{2+}. Pyrithione binds weakly to Cd^{2+}, forming a 2:1, charge-neutral complex that readily diffuses into cells [25]. Then, the medium was replaced and cells were grown under control conditions for 24 h, during which the distribution of Cd^{2+} and Zn^{2+} between proteome and MT was determined. Immediate Sephadex G-75 chromatography of the cell supernatant revealed that initially intracellular Cd^{2+} was solely bound to the proteome (Figure 7a). By 6 h, a sizable peak of Cd^{2+} associated with MT was already evident (Figure 7b) and by 24 h, almost all of the proteome-bound Cd^{2+} had been transferred to a growing MT pool (Figure 7c). Notably, mixed metal, Cd,Zn-MT was the product as seen in cells and tissues exposed to Cd^{2+} [26]. The progressive appearance of Cd,Zn-MT over time parallels what is observed when cells are exposed continuously to Cd^{2+} for 24 h [27]. Thus, it appears that in cells as well as with isolated proteome, MT can react with Cd-proteome according to reaction 8 or 9.

4. Discussion

Cell and tissue injury caused by toxic metals is commonly multi-faceted. In the case of Cd^{2+}, a so-called Fanconi syndrome results from exposure [3,4]. This conglomerate of nephrotoxic effects involves the depression of a number of Na^+-dependent nutrient transport processes that occur in the proximal tubule, including those that resorb glucose, amino acids, phosphate, and calcium from the glomerular filtrate as it is being converted to urine [3,4]. Potentially, a variety of biochemical sites may be involved in the production of these lesions. Generally, attempts to understand Cd^{2+}-based toxicity have focused on one or another of the pathological issues or underlying biochemical outcomes of exposure [10,11]. Commonly, such studies have not defined the chemical sites of binding of Cd^{2+} that initiate observed perturbations in cellular function. As such, with some exceptions research on the

mechanisms of toxicity caused by metals and metalloids lack a strong bioinorganic chemical foundation.

The present study begins an inquiry into approaches and methods that make possible proteomic-level analyses of the reactions of toxic metals and metalloids with cells. In this communication, we queried how Cd^{2+} interacts with the proteome taken as a whole. The proteome was considered as a chemical reactant and its reaction with Cd^{2+} characterized. The hypothesis was pursued that Cd^{2+} favors reaction with native Zn-binding sites within the proteome (reaction 4).

The displacement of Zn^{2+} from the Zn-proteome by Cd^{2+} was investigated by assessing whether Zn^{2+} was mobilized from the proteome upon incubation with Cd^{2+}. The reaction of Cd^{2+}-treated (Zn)-proteome with three competing ligands, ZQ, EDTA, and apo-MT, demonstrated that the presence of Cd^{2+} within the proteome labilized Zn^{2+} as measured by the production of $Zn(ZQ)^2$, Zn-EDTA, and Zn-MT, respectively (Figures 3–5). Under stoichiometric conditions of reaction, Cd^{2+} displaced a large fraction of the Zn^{2+} contained in the proteome. In turn, this implied that the equilibrium affinity of these sites for Cd^{2+} exceeded their stability with Zn^{2+}. Since stability constants favor Cd^{2+} over Zn^{2+} as the ligand coordination environment shifts from carboxylate, imidazole, and amine toward sulfhydryl groups, the results suggest that, quantitatively, sulfhydryl ligation is prominent within the Zn-proteome as seen in various types of Zn-finger proteins [13].

It was also interesting that the metal ion exchange reactions were kinetically facile. Such comparatively rapid reactions have been reported with Zn-MT and Zn-finger proteins [9,23,28,29]. But Zn-enzymes such as carboxypeptidase, superoxide dismutase, and carbonic anhydrase appear much more sluggish in their metal ion exchange chemistry [30–32].

Apo-MT demonstrates robust affinity for Zn^{2+} with an apparent stability constant at pH 7 of at least $10^{11.2}$ [16]. Nevertheless it only removed 0–10% of Zn^{2+} from the Zn-proteome (Figure 5a). This finding corroborated an earlier observation that apo-MT can co-exist with the Zn-proteome *in vivo* or *in vitro* [22]. In comparison, under similar conditions a variety of small metal chelating agents sequester 25–30% of proteomic Zn^{2+}. The reactivity of the Cd-proteome with apo-MT was remarkable when contrasted with the inertness of the native Zn-proteome to reaction with this competing ligand. An earlier study showed that rabbit apo-MT readily extracted Cd^{2+} from Cd-carbonic anhydrase and did so faster than EDTA [33]. Moreover, a synthetic peptide containing residues 49–61 of MT and the last 4 cysteinyl sulfhydryl groups of the sequence rapidly and stoichiometrically extracted Cd^{2+} from the protein [33,34]. It was argued that this peptide might serve as a model for cellular reaction of apo-MT with Cd-proteins. Being at the C-terminus of the MT peptide, where there is least steric hindrance to ligand substitution reactions and containing the only four contiguous cysteinyl sulfhydryl groups that bind to the same Cd^{2+} in Cd_7-MT, this end of the molecule is best suited to undergo direct reaction with sites that contain Cd^{2+}.

Successful inter-protein metal ion exchange reaction between Cd-proteome•Zn and Zn-MT was observed for the first time in this study (Figure 6). Previously, it had been shown that

reaction of Zn^7-MT with Cd-tramtrack, a transcription factor, restored its capacity to bind to its cognate DNA sequence [35]. Conceivably, the reaction involves the direct exchange of Cd^{2+} and Zn^{2+},

$$\mathrm{Cd-proteome \bullet Zn_a + Zn_b - MT \rightleftarrows Zn_b - proteome \bullet Zn_a + Cd - MT} \quad (10)$$

If so, that would mean that protein functionality was restored to at least some of the proteins undergoing Cd^{2+}-Zn^{2+} exchange. This is a long standing hypothesis, based on the finding in mixed metal Cd^n,Zn^{7-n}-MT that Cd^{2+} and Zn^{2+} tend to be segregated between the two metal-thiolate clusters [23,26,36]. It was contended that the C-terminal domain maintains Cd^{2+} in an inert form unavailable to sensitive sites in the cell and the N-terminal domain binds more reactive Zn^{2+} that might exchange metals with other sites. The present results do not discriminate between reaction 10 and another possible outcome,

$$\mathrm{Cd-proteome \bullet Zn_a + Zn_b - MT \rightleftarrows proteome \bullet Zn_a, Zn_b + Cd - MT} \quad (11)$$

followed possibly by

$$\mathrm{proteome \bullet Zn_a, Zn_b \rightleftarrows Zn_{(aorb)} - proteome \bullet Zn_{(bora)}} \quad (12)$$

in which apo-Zn-proteins are reconstituted with Zn^{2+}.

In principle, reactions 10 and 11 involve two fully coordinated sites that are associated with bulky proteins and are, thus, the most difficult to accomplish from a mechanistic stand point. Nevertheless, such reactions recall a signature reaction of MT in which these two metal ions are exchanged between different MT molecules and different domains according to the reaction (13) in order to achieve the mixed metal MT species observed in cells [36]:

$$\mathrm{mCd_7 - MT + nZn_7 - MT \rightleftarrows (m+n)Cd_{7m/(m+n)}, Zn_{7n/(m=n)} - MT} \quad (13)$$

The MT concentration-dependence of the reaction portrayed in Figure 6b was not determined. Still, under stoichiometric conditions, not all of the proteomic Cd^{2+} was shifted into the MT pool. It is likely that the residual Cd^{2+} bound within the proteome represents binding to sites that are unreactive with MT and contribute to cytotoxicity. As methods are developed to fractionate and analyze the Cd-proteome, attention will be focused on this pool of Cd^{2+}.

Proteomic studies were also conducted with whole cell supernatant that differs from proteome by the presence of glutathione. GSH has been considered an important contributor to cellular protection against Cd^{2+} toxicity [22]. Its presence does not alter the capacity of Cd^{2+} to react with the proteome.

To complement the chemical studies with a comparable *in vivo* model of Cd^{2+} exposure, cells were incubated with Cd^{2+} and pyrithione for 30 min during which Cd^{2+} was transported efficiently from the extracellular medium into the cells by pyrithione, which forms a 2:1 complex with Cd^{2+} that is both charge neutral and lipophilic. At the end of this period, Cd^{2+} was associated with the proteome as seen *in vitro* (Figure 7). Over time, as MT

synthesis was induced, an increasing concentration of Cd,Zn-MT appeared and the proteomic pool of Cd^{2+} declined. These results revealed for the first time that intracellular MT can compete directly and effectively with Cd^{2+} associated with the proteome just as it does *in vitro*. It has been widely hypothesized that this type of reaction occurs in cells, but heretofore it could not be distinguished from the possibility that newly synthesized MT only intercepted in-coming Cd^{2+} before it reacted with the proteome.

The cellular experiment matched porcine Cd-proteome and MT, whereas in the Cd-proteomic reactions, rabbit MT was employed. That the *in vivo* and *in vitro* reactions yielded qualitatively similar results both validates the choice of rabbit MT in this study and suggests that on a proteomic scale of analysis, small differences in non-cysteinyl amino acids within MTs do not play a major role in MT reactivity [17,18].

The cumulative results of this paper support the hypothesis that Cd^{2+} can undergo widespread reaction with the Zn-protein through metal ion exchange. In turn, it is hypothesized that facets of the diverse sorts of cell injury described for Cd^{2+} are rooted in this type of reaction. In addition, given the major role of sulfhydryl-containing sites in the trafficking of Cu^{1+}, consideration needs to be given to perturbation of the Cuproteome by Cd^{2+} [37].

The lability of proteomic Zn^{2+} to metal ion substitution by Cd^{2+} suggests that other toxic metallic species might act through their reaction with elements of the Zn-proteome. For example, preliminary experiments such as those described above, indicate that Pb^{2+} can also undergo reaction 4 and replace Zn^{2+} in proteomic binding sites. Indeed, the apparent large role of cysteinyl sulfhydryl ligands in binding proteomic Zn^{2+} strengthen the hypothesis that heavy metal and metalloid species may target the Zn-proteome.

The analytical methodology used in this study, gel filtration chromatography in combination with metal analysis by atomic absorption spectrophotometry or inductively coupled plasma mass spectrometry has been used widely to determine the concentration of metals bound collectively to the proteome [38]. In order to reveal metals bound to individual proteins, much more refined protein separation is required. Polyacrylamide gel electrophoretic (PAGE separation of proteome combined with laser ablation inductively coupled plasma mass spectrometry has shown promise [39]. But the lack of a PAGE technique that both provides high resolution protein separation and retains proteins in their native states with bound metals has hindered progress [39,40]. The authors have devised a modification of sodium dodecyl sulfate PAGE that meets both of these requirements and will soon report on its use in understanding the reaction of Cd^{2+} with the Zn-proteome.

Acknowledgements

the authors appreciate the support of NIH grants ES-04026, ES-04184 and GMS-85114.

Abbreviations

Cd,Zn-MT	metallothionein with Cd^{2+} and Zn^{2+} bound to it

DPBS	Dulbecco's phosphate buffered saline
FCS	fetal calf serum
ICP-MS	inductively coupled plasma mass spectrometry
MT	metallothionein
PAGE	polyacrylamide gel electrophoresis
ZQ	Zinquin, acid form
Zn-MT	metallothionein with Zn^{2+} bound to it

References

1. Petering, DH.; Kothini, R.; Meeusen, J.; Rana, U. Cellular and Molecular Biology of Metals. Zalups, RK.; Koropatnick, J., editors. Boca Raton: CRC Press; 2010. p. 1-34.
2. Petering DH, Krezoski S, Tabatabai N. Met. Ions in Life Sci. 2009; 5:353–398.
3. Johri N, Jacquillet G, Unwin R. Biometals. 2010; 23:783–792. [PubMed: 20354761]
4. Thévenod F, Lee WK. Met. Ions Life Sci. 2013; 11:415–490. [PubMed: 23430781]
5. Tabatabai NM, Blumenthal SS, Petering DH. Toxicology. 2005; 207:369–382. [PubMed: 15664265]
6. Kothinti RK, Blodgett AG, Petering DH, Tabatabai NM. Toxicol. Appl. Pharmacol. 2010; 244:254–262. [PubMed: 20060848]
7. Kobayashi E, Okubo Y, Suwazono Y, Kido T, Nogawa K. J. Appl. Toxicol. 2002; 22:431–436. [PubMed: 12424747]
8. Liu J, Liu Y, Habeebu SS, Klaassen CD. Toxicol. Sci. 1998:197–203. [PubMed: 9928683]
9. Kothinti R, Blodgett A, Tabatabai NM, Petering DH. Chem. Res. Toxicol. 2010; 223:405–412. [PubMed: 20073493]
10. Thévenod F. Appl. Pharmacol. 2009; 238:221–239.
11. Xiao W, Liu Y, Templeton DM. Appl. Pharmacol. 2009; 238:315–326.
12. Laity JH, Lee BM, Wright PE. Curr. Opin. Struct. Biol. 2001; 11:39–46. [PubMed: 11179890]
13. Razin SV, Borunova VV, Maksimenko OG, Kantidze OL. Biochemistry (Mosc). 2012; 77:217–226. [PubMed: 22803940]
14. Andreini C, Banci L, Bertini I, Rosato A. J. Proteome Res. 2006; 5:196–201. [PubMed: 16396512]
15. Namdarghanbari M, Wobig W, Krezoski S, Tabatabai MN, Petering DH. J. Biol. Inorg. Chem. 2011; 16:1087–1101. [PubMed: 21822976]
16. Namdarghanbari MA, Meeusen J, Bachowski G, Giebel N, Johnson J, Petering DH. J. Inorg. Biochem. 2010; 104:224–231. [PubMed: 20007001]
17. Hunziker PE, Kaur P, Wan M. Biochem. J. 1995; 306:265–270. [PubMed: 7864820]
18. Huang M-C, Pan PK, Zheng TF, Chen NC, Peng JY, Huang PC. Gene. 1998; 211:49–55. [PubMed: 9573337]
19. Nowakowski AB, Petering DH. Inorg. Chem. 2011; 50:10124–10133. [PubMed: 21905645]
20. Nasir MS, Fahrni CJ, Suhy DA, Kolodsick KJ, Singer CP, O'Halloran TV. J. Biol. Inorg. Chem. 1999; 4:775–783. [PubMed: 10631609]
21. Petering DH, Zhu J, Krezoski S, Meeusen J, Kiekenbush C, Krull S, Specher T, Dughish M. Exp. Biol. Med. (Maywood). 2006; 231:1528–1534. [PubMed: 17018876]
22. Rana U, Kothinti R, Meeusen J, Tabatabai NM, Krezoski S, Petering DH. Inorg. Biochem. 2008; 102:489–499.
23. Otvos J, Petering DH, Shaw CF III. Comments on Inorg. Chem. 1989; 9:1–35.
24. Wimmer U, Wang Y, Georgiev O, Schaffner W. Nucleic Acids Res. 2005; 33:5715–5727. [PubMed: 16221973]

25. Forbes IJ, Zalewski PD, Hurst NP, Giannakis C, Whitehouse MW. FEBS Lett. 1989; 247:445–447. [PubMed: 2785460]
26. Otvos JD, Armitage IM. Proc. Natl. Acad. Sci. U S A. 1980; 77:7094–7098. [PubMed: 6938956]
27. Blumenthal S, Lewand D, Krezoski SK, Petering DH. Toxicol. Appl. Pharmacol. 1996; 136:220–228. [PubMed: 8619229]
28. Ejnik J, Shaw CF 3rd, Petering DH. Inorg. Chem. 2010; 49:6525–6534. [PubMed: 20560649]
29. Quintal SM, dePaula QA, Farrell NP. Metallomics. 2011; 3:121–139. [PubMed: 21253649]
30. Coleman JE, Vallee BL. J. Biol. Chem. 1961; 236:2244–2249. [PubMed: 13694603]
31. Carrico RJ, Deutsch HF. J. Biol. Chem. 1970; 245:723–727. [PubMed: 4984626]
32. Coleman JE. Biochemistry. 1965; 4:2644–2655. [PubMed: 4956423]
33. Ejnik J, Muñoz A, Gan T, Shaw CF 3rd, Petering DH. J. Biol. Inorg. Chem. 1999; 4:784–790. [PubMed: 10631610]
34. Muñoz A, Laib F, Petering DH, Shaw CF 3rd. J Biol Inorg Chem. 1999; 4:495–507. [PubMed: 10555583]
35. Roesijadi G, Bogumil R, Vasák M, Kägi JH. J. Biol. Chem. 1998; 273:17425–17432. [PubMed: 9651329]
36. Nettesheim DG, Engeseth HR, Otvos JD. Biochemistry. 1985; 24:6744–6751. [PubMed: 4074725]
37. Rubino JT, Franz KJ. J Inorg Biochem. 2012; 107:129–143. [PubMed: 22204943]
38. Gómez-Ariza JL, Jahromi EZ, González-Fernández M, García-Barrera T. J. Gailer. Metallomics. 2011; 3:566–577.
39. Sussulini A, Becker JS. Metallomics. 2011; 3:1271–1279. [PubMed: 22020804]
40. Barnett JP, Scanlan DJ, Blindauer CA. Anal. Bioanal. Chem. 2012; 402:3311–3322. [PubMed: 22302168]

Highlights of this manuscript include the following

- Novel experiments reveal the reaction of the Zn-proteome with Cd^{2+}.
- Cd^{2+} displaces Zn^{2+} from Zn-proteins in approximately stoichiometric fashion.
- Much of the Zn-proteome can be converted to Cd-proteome.
- Both apo-metallothionein (MT) and Zn_7-MT bind Cd^{2+} from Cd-proteome.
- Cellular Cd-proteome reacts with MT following the induction of MT.

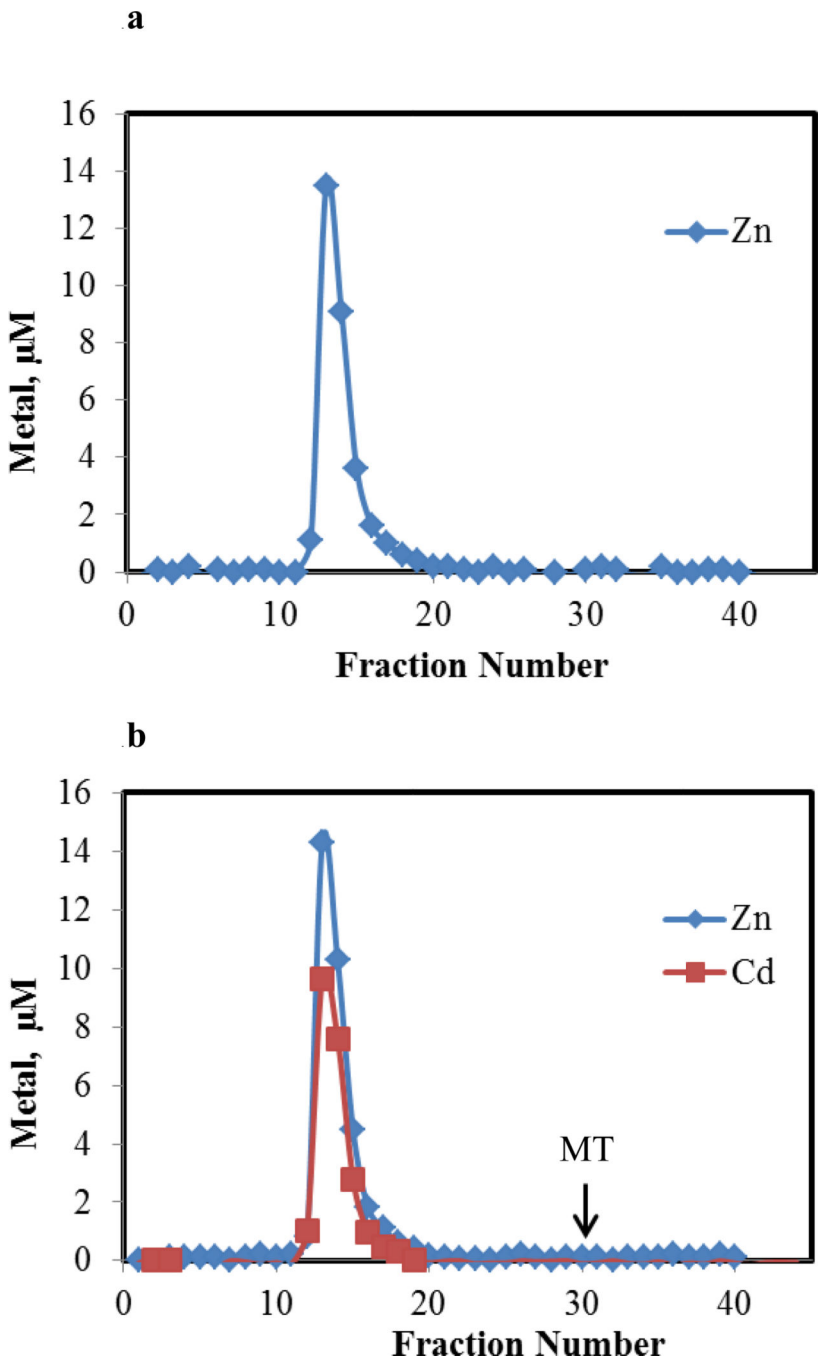

Figure 1.

Sephadex G-75 chromatography of supernatant from 5×10^7 cells. a. Distribution of Zn^{2+} in sample containing 28 μM Zn^{2+}. Arrow represents location at which Zn-MT elutes. b. Distribution of Zn^{2+} and Cd^{2+} after adding 23 μM Cd^{2+} to 28 μM Zn^{2+} present in Zn-proteome (a). Reaction time, 60 min.

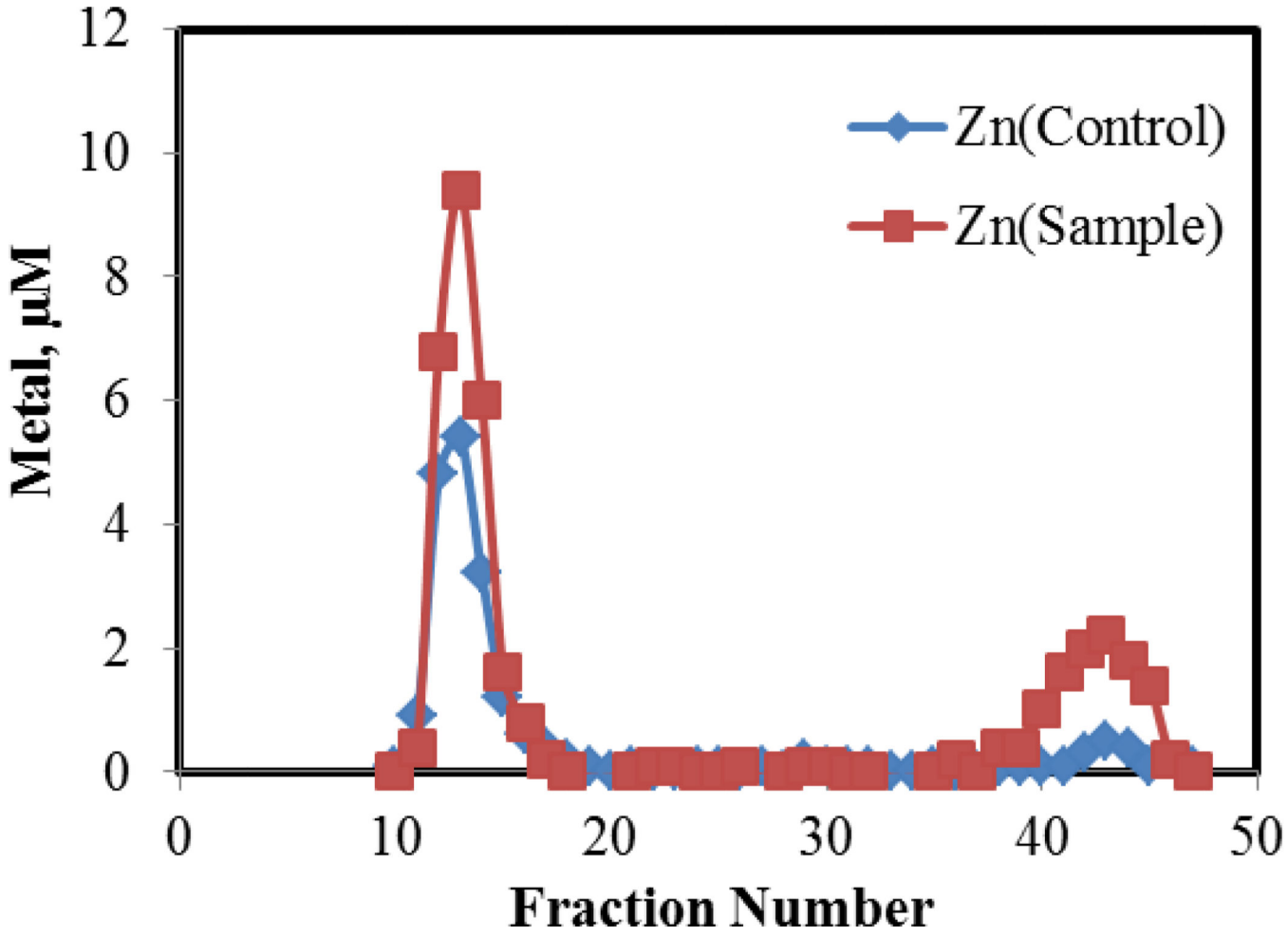

Figure 2.

Sephadex G-75 chromatography of Zn-proteome reacted with ZQ. Control (10 µM) Zn^{2+} as Zn-proteome) and Sample (10 µM Zn-proteome and 10 µM Zn^{2+} reacted with 50 µM ZQ). Reaction time, 60 min.

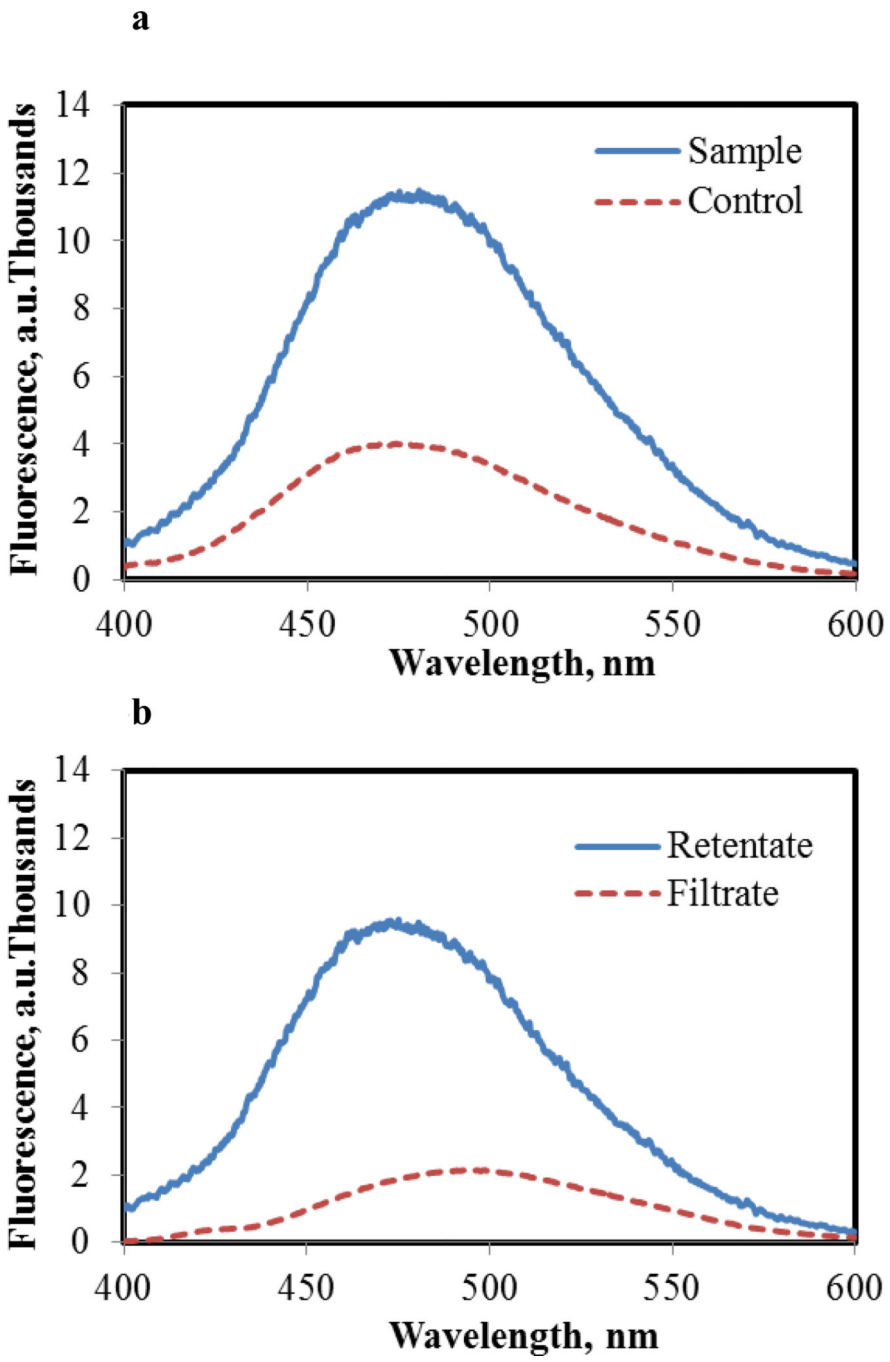

Figure 3.

Fluorescence spectra of Zn-proteome and Cd^{2+} treated Zn-proteome reacted with ZQ_{ACID}. a. Control spectrum of Zn-proteome containing 4.5 μM Zn^{2+} reacted with 15 μM ZQ_{ACID} in 20 mM degassed Tris buffer pH 7.4 (dashed line). Sample spectrum of Cd^{2+} exposed Zn-proteome containing 4.5 and 3.2 μM Zn^{2+} and Cd^{2+}, respectively, reacted with 15 μM ZQ_{ACID} in 20 mM Tris buffer pH 7.4 (solid line). Fluorescence emission spectra were recorded after 60 minutes with an excitation at 370 nm. b. Fluorescence emission spectra of

the filtrate (dashed line) and retentate (solid line) from centrifugal separation of Cd^{2+} exposed sample in a.

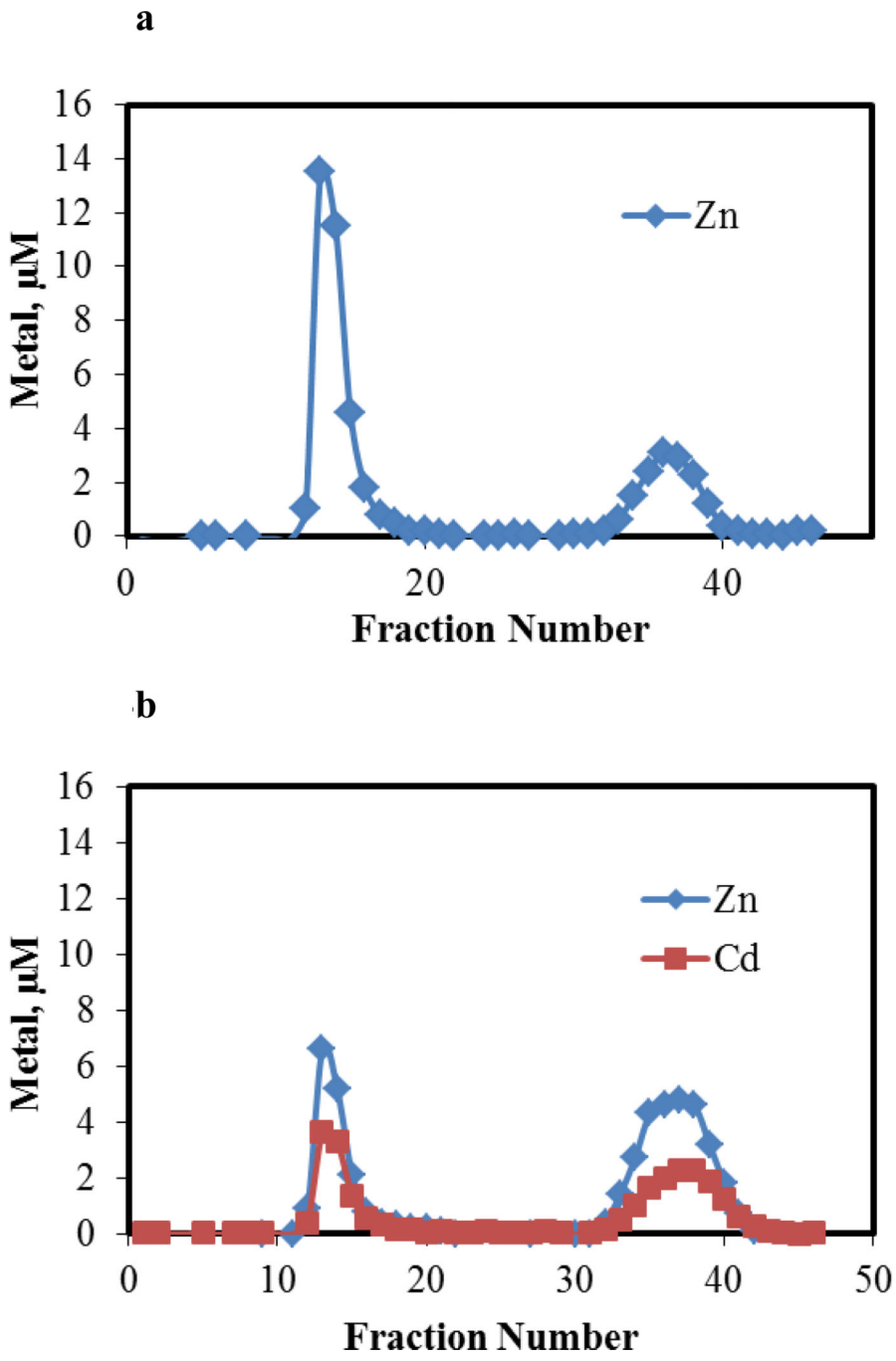

Figure 4.

Sephadex G-75 chromatography of the reaction mixture of EDTA and Cd-loaded proteome. a. Proteome containing 44 μM Zn^{2+} and b. Proteome with 44 μM Zn^{2+} and 22 μM Cd^{2+} reacted with 86 μM EDTA in 20 mM Tris buffer, 0.1 M KCl, pH 7.4. Reaction time, 60 min.

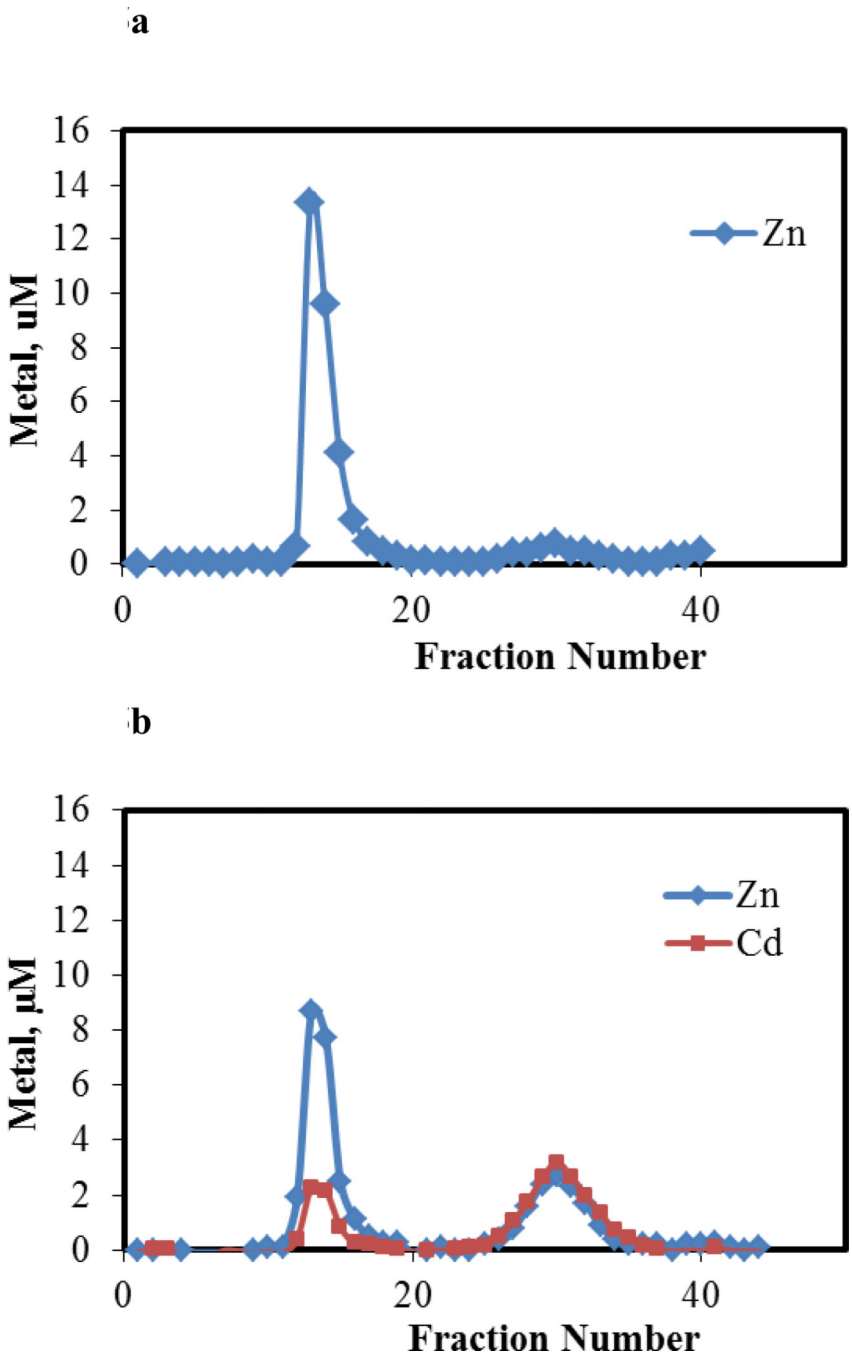

Figure 5.

Sephadex G-75 chromatography of the reaction mixture of apo-MT and Cd-loaded proteome. a. Proteome containing 28 μM Zn^{2+} and b. proteome with 28 μM Zn^{2+} and 23 nmoles μM Cd^{2+} reacted with 4 μM apo-MT (28 μM Zn^{2+} or Cd^{2+} binding capacity) in 20 mM Tris buffer, 0.1 M KCl, pH 7.4. Reaction time, 60 min.

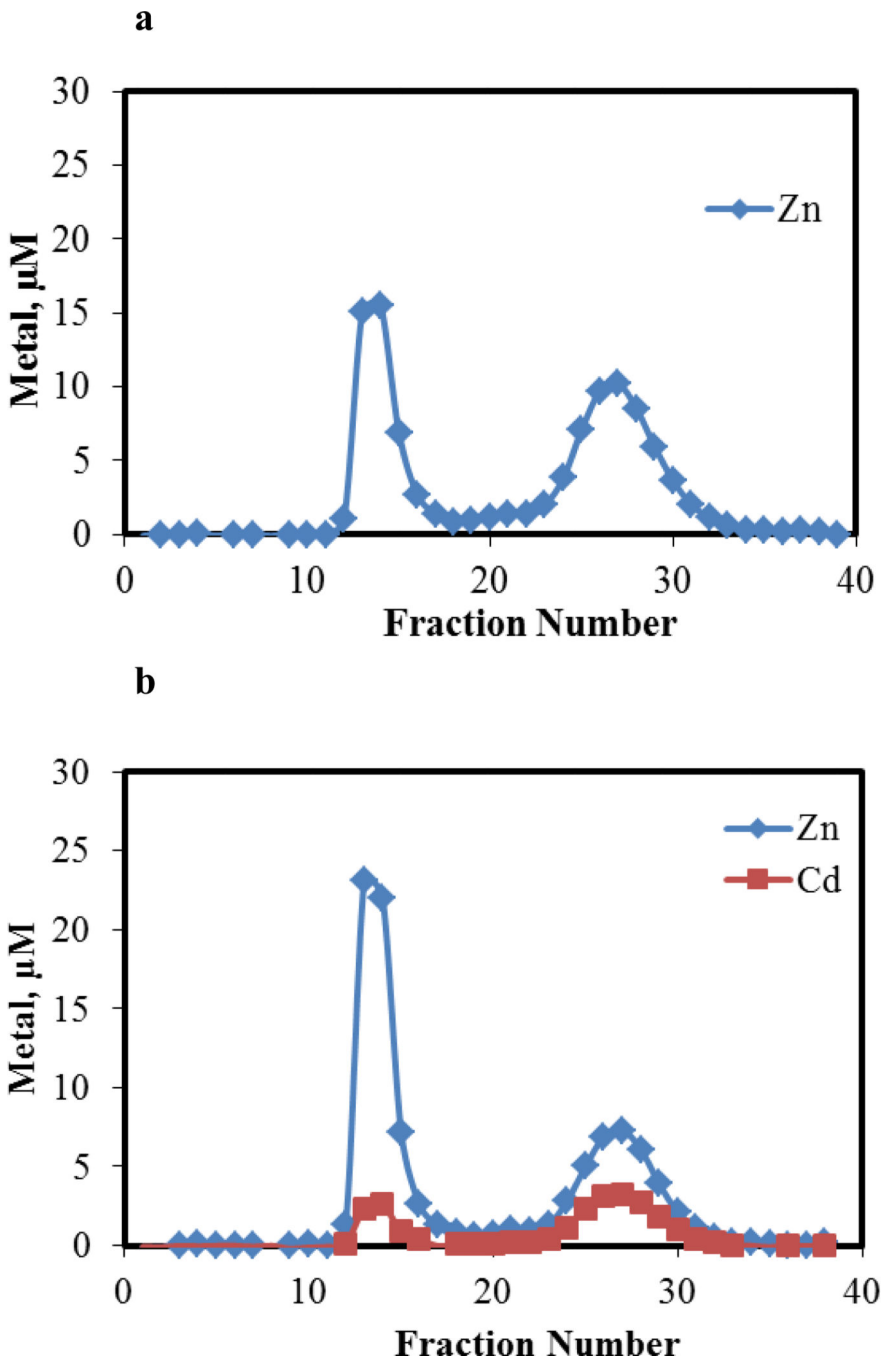

Figure 6.

Sephadex G-75 chromatography of the reaction of Zn-MT and Cd-loaded proteome. a. Proteome containing 44 µM Zn^{2+} and b. proteome with 44 µM Zn^{2+} and 25 µM Cd^{2+} reacted with Zn^{7}-MT (56 µM Zn^{2+}) in 20 mM Tris buffer, 0.1 M KCl, pH 7.4. Reaction time, 60 min.

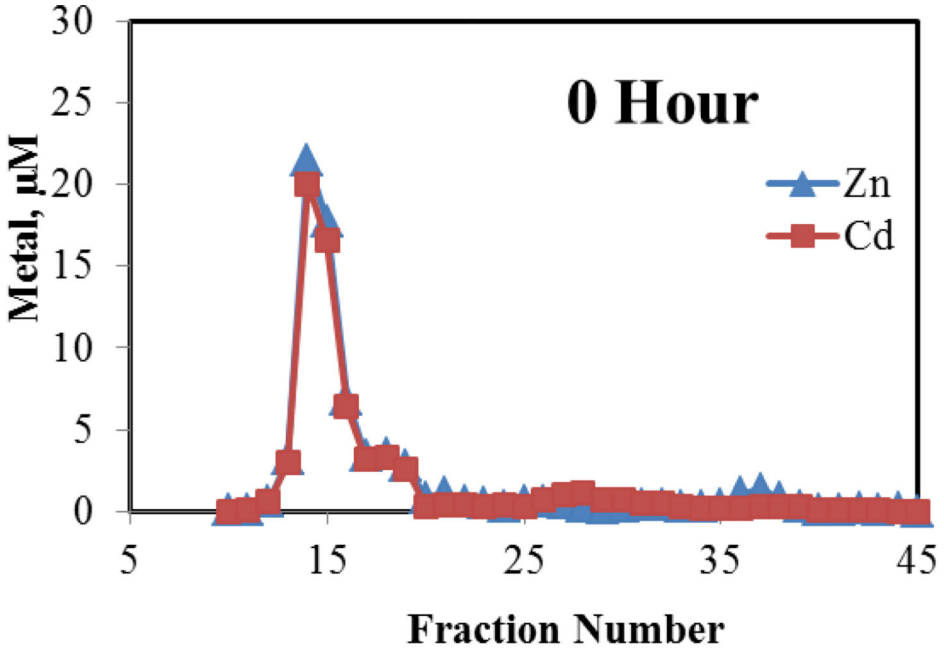

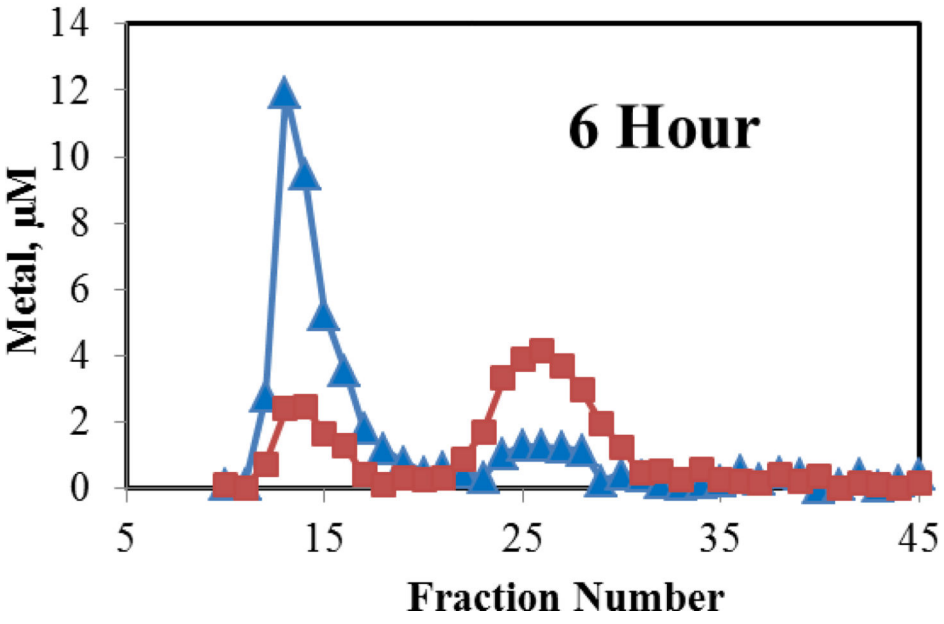

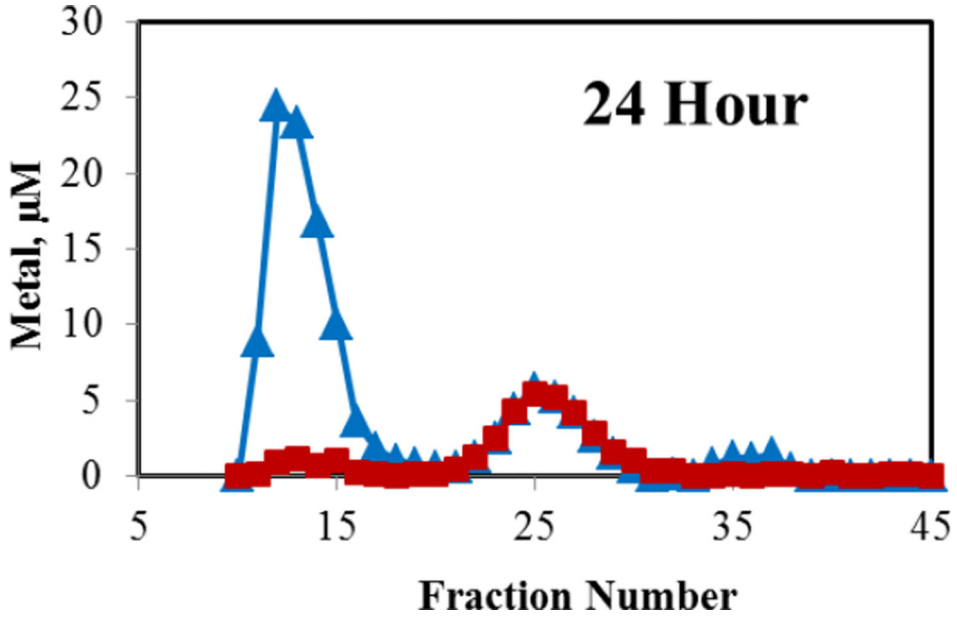

Figure 7.

Sephadex G-75 chromatography of the intracellular distribution of Cd^{2+} and Zn^{2+} after exposure of cells to Cd^{2+} plus pyrithione. Incubation of about 10^8 cells with 60 µM Cd^{2+} and 3 µM pyrithione for 30 min, preparation of cell lysates, followed by chromatography at indicated times.